Experimental Parasitology 126 (2010) 332–336

Contents lists available at ScienceDirect

Experimental Parasitology

journal homepage: www.elsevier.com/locate/yexpr

Cellular analysis of host cell infection by different developmental stages of *Trypanosoma cruzi*

Luis Florencio-Martínez [a,b], Claudia Márquez-Dueñas [a], Gilberto Ballesteros-Rodea [a,c], Santiago Martínez-Calvillo [b], Rebeca Manning-Cela [a,*]

[a] Departamento de Biomedicina Molecular, Centro de Investigación y de Estudios Avanzados del IPN, México D.F., Mexico
[b] FES Iztacala, UBIMED, UNAM, Edo. de México, Mexico
[c] Facultad de Medicina Veterinaria y Zootecnia, UNAM, Mexico

ARTICLE INFO

Article history:
Received 11 November 2009
Received in revised form 17 March 2010
Accepted 6 April 2010
Available online 28 April 2010

Keywords:
Parasites
Transfection
Green fluorescent protein
Infectivity
Epimastigotes
Trypomastigotes
Amastigotes

ABSTRACT

Trypanosoma cruzi is an obligate intracellular parasite that infects phagocytic and non-phagocytic mammalian cells by a complex process that appears to involve several discrete steps. Even though the infection process was described many years ago, the molecular mechanisms involved remain poorly understood. As fluorescent proteins have proven to be excellent tools for live-cell imaging, we used *EGFP*- and *DsRed1-1*-transfected trypomastigotes, amastigotes and epimastigotes to study the infection process in living cells. Contrary to what has been reported, our results showed that epimastigotes are as infective as trypomastigotes and amastigotes. Besides, differences in replication, differentiation and parasite release times were observed among the stages. Our results suggest that the different developmental stages use distinct attachment and invasion mechanisms. We propose that fluorescent-based plasmid expression systems are good models for studying the infection process of intracellular microorganisms and could offers insights about the molecular mechanisms involved.

1. Introduction

Trypanosoma cruzi is the flagellated protozoan causative agent of Chagas' disease, an incurable fatal illness that affects 20 million people on the American Continent (Barrett et al., 2003). This parasite has a complex life cycle involving three distinct developmental stages that alternate between the invertebrate and the vertebrate hosts. Although the basic features of the infection process have been known for a century, diverse aspects of the molecular mechanisms involved have only recently been elucidated, and others aspects remain either controversial or unstudied (Espinoza and Manning-Cela, 2007). In humans as an obligate intracellular parasite, *T. cruzi* infects many different phagocytic and non-phagocytic cells through a complex cycle characterized by the presence of several discrete steps (attachment, invasion, multiplication, differentiation and parasite release from the host cell), the participation of multiple parasites and host cell molecules and the activation of bidirectional signaling cascades (Espinoza and Manning-Cela, 2007). In non-phagocytic cells, where disease pathogenesis takes place, some progress has been made in understanding the process of trypomastigote attachment and internalization into the host cell (Andrade and Andrews, 2005). Conversely, the available information about amastigotes is comparatively scarcer than that for trypomastigotes, and nothing is known about epimastigotes. Moreover, diverse aspects and key questions of the parasite escape from the parasitophorous vacuole, the parasite differentiation before and after the amastigote multiplication in the cytosol and the trypomastigote exit from the host cell remain poorly understood or unstudied (Espinoza and Manning-Cela, 2007). In the present work, we established the fluorescence-based monitoring of *in vitro* infections initiated with trypomastigotes, amastigotes and epimastigotes that were stably transfected with EGFP- and DsRed1-1-based plasmid expression systems, to study the infection kinetics of the different developmental forms of *T. cruzi*. Furthermore, the analysis of replication, differentiation and parasite release kinetics is also presented.

2. Experimental procedures

2.1. Cells and parasites

NIH 3T3 fibroblasts were grown in Dulbecco's minimal essential medium (DMEM) supplemented with 10% fetal bovine serum (FBS), 1% glutamine and 5 mg/ml of penicillin–streptomycin at

* Corresponding author. Address: Av. IPN 2508, Col. San Pedro Zacatenco, C.P. 0736, México D.F., Mexico. Fax: +52 5557473938.
E-mail address: rmanning@cinvestav.mx (R. Manning-Cela).

0014-4894/$ - see front matter © 2010 Elsevier Inc. All rights reserved.
doi:10.1016/j.exppara.2010.04.015

37 °C in a humidified atmosphere containing 5% CO_2. Epimastigotes from the *T. cruzi* CL-Brenner strain and transfected lines were maintained in liver infusion tryptose (LIT) medium containing 10% FBS and 0.1 mg/ml hemine at 28 °C. The trypomastigotes and amastigotes were obtained from the supernatant of the NIH 3T3 monolayers infected as described below. The amastigotes were separated from trypomastigotes using the amastigote-specific antibody 2C2B6 against the Ssp-4 surface antigen of amastigotes, as previously described (Manning-Cela et al., 2001).

2.2. Construction of pTREXn–EGFP and pTREXn–DsRed1-1

The *EGFP* and *DsRed1-1* sequences were obtained by the digestion of pEGFP-N1 and pDsRed1-1 (Clontech) with *Hind*III/*Not*I and *Eco*RI/*Not*I, respectively, and after gel purification were sub-cloned in pTREXn (Vazquez and Levin, 1999) in the corresponding restriction enzymes sites. The resulted plasmids, pTREXn–EGFP and pTREXn–DsRed1-1, were used for transfection experiments after verifying the correct cloning by sequence analysis.

2.3. Generation of fluorescent parasites

Mid-log phase epimastigotes (3×10^8) resuspended in cold LYT medium were transfected by electroporation (BTX ECM 830) with 100 μg of cesium chloride-purified plasmid DNA at 300 V for 12 ms in 2 mm BTX electroporation cuvettes. After electroporation the transfected parasites were maintained for 5 min at 4 °C and then transferred to a fresh complemented LIT medium and incubated at 28 °C. After 48 h, the parasites were exposed to antibiotic selection with 500 μg/ml of G418 (No. Cat. 10131-035/GIBCO). Once antibiotic-resistant growth cultures were established, fluorescence clonal derivatives were isolated from each EGFP and DsRed1-1 parasite population by flow cytometry (FACSVantage, Becton, Dickinson).

2.4. Infectivity assay

For primary infections, monolayers of NIH 3T3 cells grown to 50% confluency in DMEM supplemented with 2% fetal calf serum were infected with 2×10^6 mid-log-phase fluorescent epimastigotes per ml, cultured in LIT media plus 10% FBS at 28 °C. Forty-eight hours later the cells were washed, and they were subsequently washed every 2 days with DMEM to remove non-adherent parasites, after which fresh DMEM plus 2% fetal calf serum was added. For the secondary infection experiments, 1×10^5/ml or 2×10^6/ml fluorescent epimastigotes cultured in LIT medium, or 1×10^5/ml or 2×10^6/ml fluorescent trypomastigotes or amastigotes obtained from the first infection and purified as described above, were used to infect NIH 3T3 fibroblasts (grown to 50% confluency) over 2 h. The cultures were washed with DMEM until non-adherent parasites were removed and fresh DMEM plus 2% fetal calf serum was added. Infections were monitored daily, and the number of amastigotes and trypomastigotes in the supernatant was determined. Using an inverted Olympus fluorescence microscope, the percentage of infected cells was calculated by comparing the number of cells containing parasites to the total number of cells, following the replication, differentiation and parasite-realized kinetics.

2.5. Epifluorescence and confocal microscopy

Cells grown over cover-slides were infected as described above and processed for fluorescence microscopy. The samples were fixed with 4% formaldehyde/PBS for 20 min, stained with 0.01 U/μl of rhodamine phalloidin (No. Cat. R415/Molecular Probes, Invitrogene) at room temperature for 20 min, nucleus was contra-stained with 5 μg/ml of DAPI (Molecular Probes), washed with PBS and mounted with vectashield® Mounting Medium (Vector Laboratories Cat. H-1000). The samples were analyzed in an Olympus fluorescence microscope BX41 equipped with a 60×/1.25 Oil Iris Ph3 UPlanFL N objective, and the images were captured with an Evolution VF Fast Cooled Color Media Cybernetics camera and analyzed with the Image-Pro Plus V 6.0 Media Cybernetics program. Besides, confocal laser microscope (Leica SP5, DM 16000, Mo) equipped with an HCXPLAPO lambda blue 63 × 1.4 NA oil objective was used and the images captured and analyzed using the software LAS AF (*Leica Application Suite Advanced Fluorescence Lite*/1.7.0 build 1240 Leica Microsystems).

2.6. Growth curves

The cultures were initiated with 1×10^6 epimastigotes per ml of complemented LIT medium incubated at 28 °C. The number of parasites was determined by direct counting with a Neubauer chamber every 24 h to determine the growing parasites. The viability of the cells was determined using the trypan blue exclusion test.

3. Results and discussion

3.1. Cloning and EGFP- and DsRed1-1-transfected parasite generation

To obtain green and red fluorescently tagged parasites, *EGFP* and *DsRed1-1* sequences were sub-cloned in the *T. cruzi*-derived cloning vector pTREXn and transfected into epimastigotes of the CL-Brenner strain, as described in Section 2. As shown in Fig. 1, epimastigotes expressing the EGFP or DsRed1-1 protein were uniformly fluorescent throughout the parasite body and flagellum as previously reported (Guevara et al., 2005; Pires et al., 2008). These results indicate that *EGFP*- and *DsRed1*-transfected parasites expressed the fluorescent proteins and demonstrate the successful generation of the florescent knock-in lines.

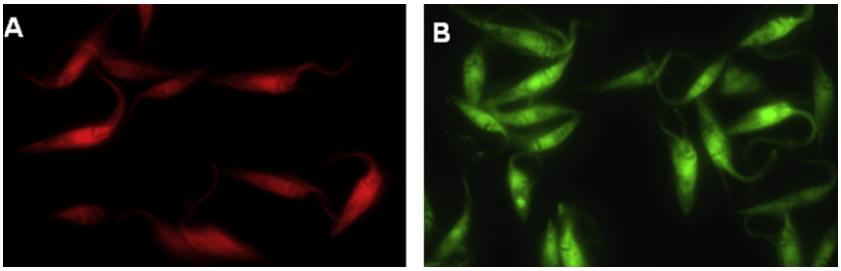

Fig. 1. Epifluorescence analysis of green and red fluorescently tagged epimastigotes. Direct observation of EGFP (A) and DsRed1-1 (B) knock-in parasites. Magnification is 60×.

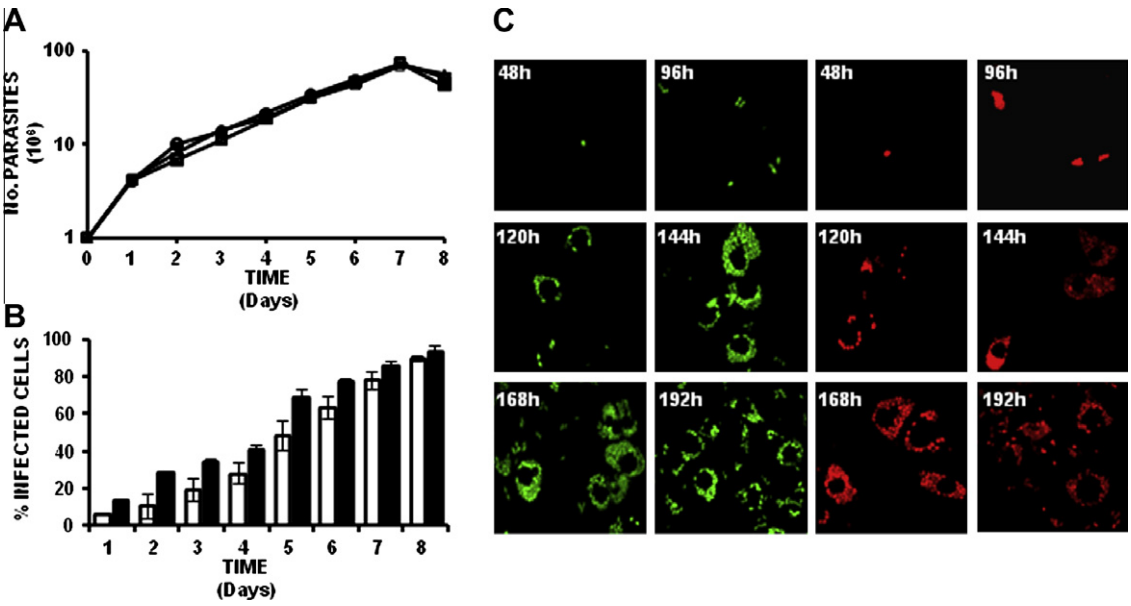

Fig. 2. The expression of fluorescent proteins did not affect cell growth or *in vitro* infectivity of epimastigotes. Growth curves (A) of the epimastigotes –▲– wt, –●– EGFP and –□– DsRed1-1 were determined as described in Section 2. NIH 3T3 fibroblasts were infected (B) with EGFP (open bars) or DsRed1-1 (gray bars) epimastigotes, and the infections were monitored, determining the number of cells containing parasites with respect to the total number of cells. The results shown are the average of three independent experiments. Direct observation (C) of cells infected with epimastigotes expressing the exogenous EGFP (green) or DsRed1-1 (red) fluorescent proteins. The evaluated time indicated in the left upper corner corresponds to the hours (h) post-infection. Magnification is 40×.

3.2. The expression of EGFP and DsRed1-1 sequences did not affect the parasite growth and its infectivity

To evaluate if the expression of fluorescence markers affect the epimastigote growth and parasite infectivity, we measured the culture growth and primary infection kinetics of EGFP- and DsRed1-1-transfected epimastigotes. As shown in Fig. 2A, no differences in growth were observed between the green and red fluorescently tagged parasites in comparison with the wild type (wt) cells, demonstrating that the fluorescent markers are innocuous. Furthermore the *EGFP*- and *DsRed1-1*-tagged parasites were able to generate productive infections in which the fluorescent proteins were found expressed throughout the entire infection process and in the different developmental stages of *T. cruzi* (Fig. 2B and C). These results are in agreement with previous reports demonstrating that these fluorescent proteins do not show any toxic effect on stably transfected cell lines and parasite strains (Guevara et al., 2005; Matz et al., 1999; Pires et al., 2008). Since many epimastigotes were differentiated to infective trypomastigotes or amastigotes during the 48 h of host cells-parasite interaction, we could do not determine if the epimastigotes were able to infect fibroblast in the primary infections.

3.3. Trypomastigotes, amastigotes and epimastigotes infect NIH 3T3 fibroblasts at similar rates in secondary infections

As green and red fluorescently tagged parasites were able to generate primary productive infections, EGFP and DsRed1-1 trypomastigotes and amastigotes were purified from infected cell supernatants. Secondary infection kinetics were then carried out using two different inoculums (1×10^5 and 2×10^6 parasites/ml/2 h) of fluorescently tagged epimastigotes, trypomastigotes and amastigotes, and the number of infected cells, the transformation from trypomastigotes and epimastigotes into amastigotes, the multiplication of intracellular amastigotes, the transformation from amastigotes to trypomastigotes and the parasites released to the supernatant were determined across time. The infection kinetics using the two different inoculums were similar for both EGFP and DsRed1-1 parasites, with lower infection levels obtained with the smaller inoculums, as expected (data not shown). The three different developmental stages induced productive infections with similar kinetics; however, differences at early times were detected (Fig. 3). The establishment of the infection was delayed when the infections were initiated with trypomastigotes and epimastigotes in comparison with amastigotes (Fig. 3B and

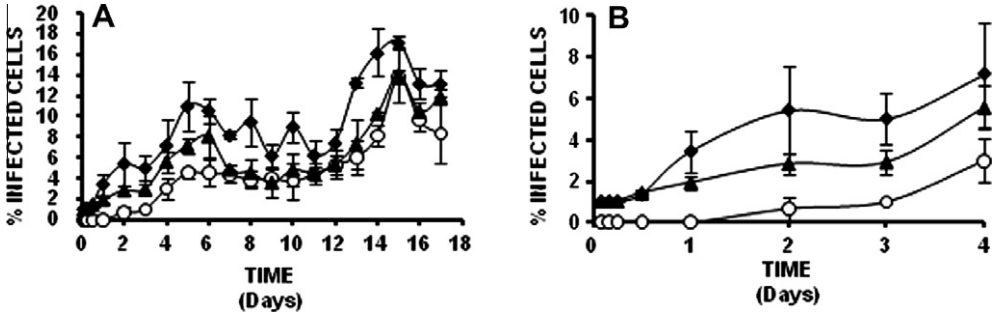

Fig. 3. Trypomastigotes, amastigotes and epimastigotes induced productive infections in 3T3 NIH fibroblasts. The cells were infected with –♦– trypomastigotes, –▲– amastigotes or –○– epimastigotes, and the infections were monitored across 18 days (A) as described in Section 2. The magnification of the first 4 days of the infection kinetics is shown in B. The results shown are the averages of three independent experiments.

Table 1
Quantitative analysis of secondary infections kinetics initiated with the different developmental forms of *T. cruzi*.

Parasite stage	Intracellular parasites (h)	Transformation into amastigotes (h)	Amastigote multiplication (h)	Amastigote transformation into trypomastigotes (h)	Parasite release to culture supernatant (h)
Trypomastigotes	2	2	24	96	168
Amastigotes	2	–	4	96	168
Epimastigotes	4	24	48	144	216

The times were determined after 2 h post-infection.
The results are the average of three independent experiments.

Table 1). As shown in Table 1, trypomastigotes and amastigotes were observed inside the host cell within the first 2 h post-infection, whereas epimastigotes were detected at 4 h post-infection. This behavior impacted the parasite transformation to amastigotes and the cell multiplication, since the parasites were shown as amastigotes after 2 h and 24 h when the infections were initiated with trypomastigotes and epimastigotes, respectively. Also, the beginning of amastigote multiplication was different between infections using amastigotes (4 h), trypomastigotes (24 h) or epimastigotes (48 h). These results showed a lag phase between trypomastigote (2 h) and epimastigote (20 h) invasion and their differentiation to amastigotes. Additionally, a lag phase was also found between differentiated parasites (22 h for trypomastigotes and 24 h for epimastigotes) and the start of amastigote multiplication, in contrast to the amastigotes, which immediately initiated replication (Table 1). The lag phase of trypomastigote transformation into amastigotes and the direct replication of amastigotes have been previously reported (Ley et al., 1988, 1990). However, the molecules and biologic mechanisms involved are still unidentified, and nothing is known about epimastigotes. In contrast to previous reports determining that epimastigotes can enter into macrophages but are destroyed (Nogueira and Cohn, 1976) and unable to infect fibroblasts (Piras et al., 1982) or HeLa cells (Manque et al., 2003), our results indicated that this developmental stage is able to attach, invade, multiply and generate productive infections in 3T3 NIH fibroblasts (Figs. 2–4). The possibility that epimastigotes were differentiated to trypomastigotes or amastigotes before invading the host cell was discarded because non-differentiated epimastigotes were seen during the 2 h parasite-cell interaction; epimastigotes were seen invading host cells (Fig. 4), and longer times than the ones used in the secondary infections have been reported as necessary for transforming epimastigotes into the infective trypomastigote and amastigote stages (Manning-Cela et al., 2001). Further support was obtained when we analyzed the infection kinetics, which clearly show differential behaviors between stages that apparently reflect stage-specific lag phases; this represents, at least in part, the time necessary for the parasite transformation into intracellular amastigotes (Fig. 3B and Table 1). The differentiation from amastigotes into trypomastigotes was also stage-delayed, where in the infections initiated with epimastigotes this step took 144 h, but with trypomastigotes and amastigotes it took 96 h. Finally, the parasite release to the culture supernatant occurred later in the infection initiated with epimastigotes (216 h) in comparison with those from amastigotes and trypomastigotes (168 h).

Our results suggest that the three different developmental forms of *T. cruzi* are infective forms that apparently engage stage-specific mechanisms to infect 3T3 NIH fibroblasts. It has been reported that trypomastigotes and amastigotes are able to infect phagocytic and non-phagocytic cells using different molecular mechanisms to invade cells and to escape from the parasitophorous vacuole (Andreoli and Mortara, 2003; Ley et al., 1988; Mortara, 1991; Mortara et al., 2005; Procopio et al., 1999, 1998; Stecconi-Silva et al., 2003). These two developmental forms mobilize bidirectional specific interacting components and signaling pathways that are apparently cell type-, parasite developmental form- and

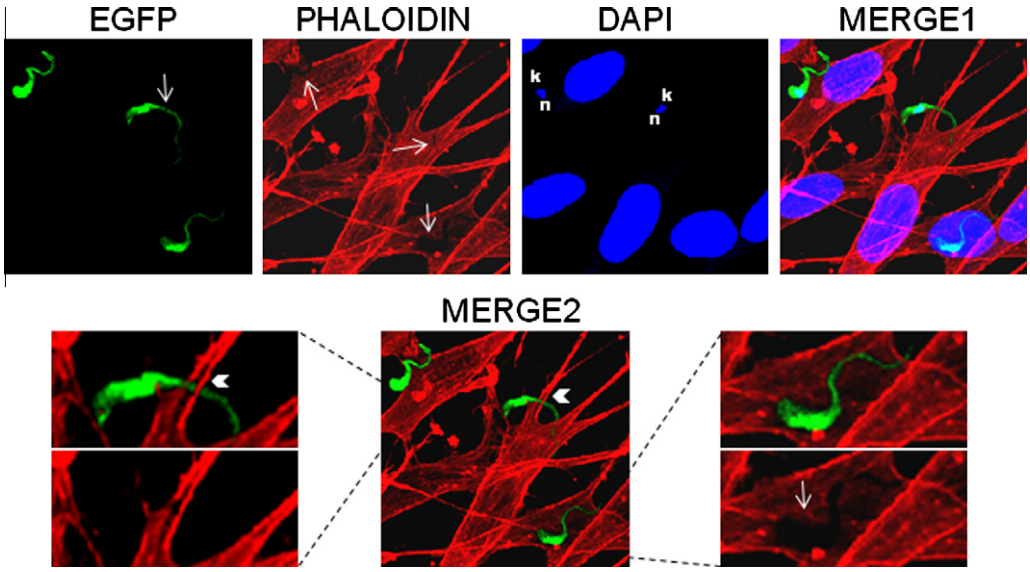

Fig. 4. The epimastigotes penetrated 3T3 NIH fibroblasts. Direct observation of extracellular and intracellular EGFP-tagged epimastigotes by confocal microscopy. The sample was stained with rhodamine phalloidin and counterstained with DAPI to visualize actin cytoskeleton (PHALOIDIN) and nuclear (n) and kinetoplast (k) DNA (DAPI), respectively. Merged images of EGFP, PHALOIDIN and DAPI (MERGE1) or EGFP and PHALOIDIN (MERGE2). Arrows indicate the parasite footprint in the host cell actin cytoskeleton and the actin fibers footprint in the parasite flagellum demonstrating that epimastigotes are capable to invade the host cells. Arrowhead indicates host cell actin fibers surrounding the parasite flagellum. Dotted lines indicate a parasite magnification. Magnification is 63×.

parasite strain-dependent (Mortara et al., 1999; Procopio et al., 1999). Therefore, it could be possible that the epimastigotes, shown to be as infective as trypomastigotes and amastigotes and having distinct surface molecules, can also use different molecular mechanisms to infect target cells. This raises questions about the biologic implications that this infective form may have during the infection of different target cells in several mammalian species and the impact that it could have in the maintenance and transmission of the infection. As epimastigotes are present in the insect feces, our observations are of relevance in understanding the molecular mechanisms involved in the efficient establishment of Chagas disease pathogenesis and likely complicate the development of *T. cruzi* infection control strategies.

The experimental fluorescence-based monitoring model reported in this work provides an useful system for *in vitro* infection studies that could provide insight into diverse aspects and key questions of the *T. cruzi* infection process which so far remains poorly understood and understudied, and supply a valuable system that could be useful for future *in vivo* infection studies.

Acknowledgments

This work was supported by the CONACYT Grants No. 42862 and 60152 awarded to R.G. Manning-Cela. G. We thank Norma Andrews (Yale University) for the generous gift of 2C2B6 antibodies, Ivan Galván for guidance during the confocal microscopy analysis and Palmira Guevara for the generous gift of pTREXn plasmid.

References

Andrade, L.O., Andrews, N.W., 2005. The *Trypanosoma cruzi*-host-cell interplay: location, invasion, retention. Nature Reviews 3, 819–823.

Andreoli, W.K., Mortara, R.A., 2003. Acidification modulates the traffic of *Trypanosoma cruzi* trypomastigotes in Vero cells harbouring *Coxiella burnetii* vacuoles. International Journal for Parasitology 33, 185–197.

Barrett, M.P., Burchmore, R.J., Stich, A., Lazzari, J.O., Frasch, A.C., Cazzulo, J.J., Krishna, S., 2003. The trypanosomiases. Lancet 362, 1469–1480.

Espinoza, G.B., Manning-Cela, R.G., 2007. An overview of mammalian cell infection by *Trypanosoma cruzi*: cellular and molecular basis. Advances in the Immunobiology of Parasitic Diseases. Kerala, India, 291–311.

Guevara, P., Dias, M., Rojas, A., Crisante, G., Abreu-Blanco, M.T., Umezawa, E., Vazquez, M., Levin, M., Añez, N., Ramirez, J.L., 2005. Expression of fluorescent genes in *Trypanosoma cruzi* and *Trypanosoma rangeli* (Kinetoplastida: Trypanosomatidae): its application to parasite-vector biology. Journal Medical Entomology 42 (1), 48–56.

Ley, V., Andrews, N.W., Robbins, E.S., Nussenzweig, V., 1988. Amastigotes of *Trypanosoma cruzi* sustain an infective cycle in mammalian cells. The Journal of Experimental Medicine 168, 649–659.

Ley, V., Robbins, E.S., Nussenzweig, V., Andrews, N.W., 1990. The exit of *Trypanosoma cruzi* from the phagosome is inhibited by raising the pH of acidic compartments. The Journal of Experimental Medicine 171, 401–413.

Manning-Cela, R., Cortes, A., Gonzalez-Rey, E., Van Voorhis, W.C., Swindle, J., Gonzalez, A., 2001. LYT1 protein is required for efficient in vitro infection by *Trypanosoma cruzi*. Infection and Immunity 69, 3916–3923.

Manque, P.M., Neira, I., Atayde, V.D., Cordero, E., Ferreira, A.T., da Silveira, J.F., Ramirez, M., Yoshida, N., 2003. Cell adhesion and Ca2+ signaling activity in stably transfected *Trypanosoma cruzi* epimastigotes expressing the metacyclic stage-specific surface molecule gp82. Infection and Immunity 71, 1561–1565.

Matz, M.V., Fradkov, A.F., Labas, Y.A., Savitsky, A.P., Zaraisky, A.G., Markelov, M.L., Lukyanov, S.A., 1999. Fluorescent proteins from nonbioluminescent *Anthozoa* species. Nature Biotechnology 17, 969–973.

Mortara, R.A., 1991. *Trypanosoma cruzi*: amastigotes and trypomastigotes interact with different structures on the surface of HeLa cells. Experimental Parasitology 73, 1–14.

Mortara, R.A., Procopio, D.O., Barros, H.C., Verbisck, N.V., Andreoli, W.K., Silva, R.B., da Silva, S., 1999. Features of host cell invasion by different infective forms of *Trypanosoma cruzi*. Memorias do Instituto Oswaldo Cruz 94 (Suppl. 1), 135–137.

Mortara, R.A., Andreoli, W.K., Taniwaki, N.N., Fernandes, A.B., Silva, C.V., Fernandes, M.C., L'Abbate, C., Silva, S., 2005. Mammalian cell invasion and intracellular trafficking by *Trypanosoma cruzi* infective forms. Anais da Academia Brasileira de Ciencias 77, 77–94.

Nogueira, N., Cohn, Z., 1976. *Trypanosoma cruzi*: mechanism of entry and intracellular fate in mammalian cells. The Journal of Experimental Medicine 143, 1402–1420.

Piras, M.M., Piras, R., Henriquez, D., Negri, S., 1982. Changes in morphology and infectivity of cell culture-derived trypomastigotes of *Trypanosoma cruzi*. Molecular and Biochemical Parasitology 6, 67–81.

Pires, S.F., Da Rocha, W.D., Freitas, J.M., Oliveira, L.A., Kitten, G.T., Machado, C.R., Pena, S.D.J., Chiari, E., Macedo, A.M., Teixeira, S.M.R., 2008. Cell culture and animal infection with distinct *Trypanosoma cruzi* strains expressing red and green fluorescent proteins. International Journal for Parasitology 38, 289–297.

Procopio, D.O., da Silva, S., Cunningham, C.C., Mortara, R.A., 1998. *Trypanosoma cruzi*: effect of protein kinase inhibitors and cytoskeletal protein organization and expression on host cell invasion by amastigotes and metacyclic trypomastigotes. Experimental Parasitology 90, 1–13.

Procopio, D.O., Barros, H.C., Mortara, R.A., 1999. Actin-rich structures formed during the invasion of cultured cells by infective forms of *Trypanosoma cruzi*. European Journal of Cell Biology 78, 911–924.

Stecconi-Silva, R.B., Andreoli, W.K., Mortara, R.A., 2003. Parameters affecting cellular invasion and escape from the parasitophorous vacuole by different infective forms of *Trypanosoma cruzi*. Memorias do Instituto Oswaldo Cruz 98, 953–958.

Vazquez, M.P., Levin, M.J., 1999. Functional analysis of the intergenic regions of TcP2beta gene loci allowed the construction of an improved *Trypanosoma cruzi* expression vector. Gene 239, 217–225.